

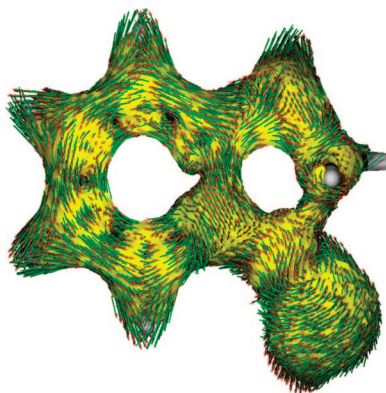
Computational Analysis on the Dual Reactivity of Conjugated “Ene-Ene-Yne” Systems

Sean P. McClintock,[†] Laura D. Shirtcliff,[†] Rainer Herges,^{*,‡} and Michael M. Haley^{*,†}

Department of Chemistry, University of Oregon, Eugene, Oregon 97403-1253, and Institut für Organische Chemie, Universität Kiel, 24098 Kiel, Germany

rherges@oc.uni-kiel.de; haley@uoregon.edu

Received June 25, 2008



The design of new reactions that yield benzo-fused five- or six-membered rings arising from conjugated ene-ene-yne precursors was examined computationally. Inclusion of heteroatoms (particularly N) in the bond making position was shown to lower activation energies due to participation of the lone pair electrons in the cyclization reactions. By systematically varying the atomic configuration in the ene-ene-yne system, the influence of heteroatoms was used to identify optimal candidates for future experimental study.

Introduction

Our laboratory has been investigating the experimental and computational cyclizations of conjugated “ene-ene-yne”, namely, azo-ene-yne^{1–4} and azo-ene-nitrile⁵ systems, for several years. The initial discovery that *o*-ethynylphenyltriazenes (**1**, Figure 1) could cyclize to form either five- or six-membered rings^{1a} (**2** and **3**, respectively) was of great interest because of the important role that heterocyclic compounds

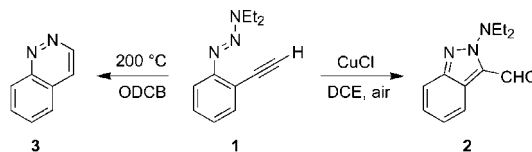


FIGURE 1. Dual reactivity of triazene **1**.

play in a wide range of chemistries.^{6–8} The ability of this one precursor to afford two different aromatic heterocycles in high yield by changing reaction conditions led us to explore further the potential of the ene-ene-yne core in the synthesis of additional heterocyclic compounds. Density functional theory (DFT) computations have been instrumental in these studies to help understand reactivity patterns, elucidate

[†] University of Oregon.

[‡] Universität Kiel.

(1) (a) Kimball, D. B.; Hayes, A. G.; Haley, M. M. *Org. Lett.* **2000**, *2*, 3825–3827. (b) Kimball, D. B.; Weakley, T. J. R.; Herges, R.; Haley, M. M. *J. Am. Chem. Soc.* **2002**, *124*, 13463–13473. (c) Kimball, D. B.; Herges, R.; Haley, M. M. *J. Am. Chem. Soc.* **2002**, *124*, 1572–1573. (d) Kimball, D. B.; Weakley, T. J. R.; Haley, M. M. *J. Org. Chem.* **2002**, *67*, 6395–6405.

(2) Shirtcliff, L. D.; Weakley, T. J. R.; Haley, M. M.; Herges, R.; Kohler, F. *J. Org. Chem.* **2004**, *69*, 6979–6985.

(3) Shirtcliff, L. D.; Hayes, A. G.; Haley, M. M.; Kohler, F.; Hess, K.; Herges, R. *J. Am. Chem. Soc.* **2006**, *128*, 9711–9721.

(4) Shirtcliff, L. D.; Haley, M. M.; Herges, R. *J. Org. Chem.* **2007**, *72*, 2411–2418.

(5) Shirtcliff, L. D.; Rivers, J.; Haley, M. M. *J. Org. Chem.* **2006**, *71*, 6619–6622.

(6) (a) Katritzky, A. R.; Pozharskii, A. F. *Handbook of Heterocyclic Chemistry*; Elsevier Science Ltd.: Oxford, 2000. (b) Joule, J. A.; Mills, K. *Heterocyclic Chemistry*; Blackwell: Oxford, U.K., 2000. (c) Li, J. J.; Gribble, G. W. *Palladium in Heterocyclic Chemistry*; Permonon: Amsterdam, 2000. (d) Eicher, T.; Hauptmann, S. *The Chemistry of Heterocycles: Structure, Reactions, Syntheses, and Application*; Wiley-VCH: Weinheim, Germany, 2003.

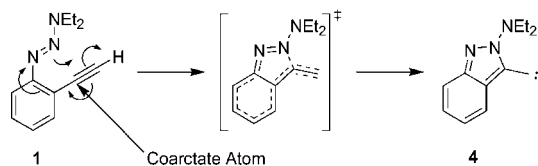


FIGURE 2. Coarctate reactivity of triazene 1.

mechanisms, and identify viable motifs for these uncommon transformations.

The formation of the five-membered ring product is quite unusual in that it proceeded through an intermediate composed of an isoindazole ring with an exocyclic carbene (**4**, Figure 2).¹ This is characteristic of coarctate reactivity as initially outlined by Herges.^{9,10} After completing a systematic classification of thousands of transformations, Herges determined that fragmentations and cyclizations involving a five-membered aromatic ring with an exocyclic carbene, among others, fell under a previously undescribed class of concerted reactions. The transition states are formally derived from pericyclic reactions, and hence proceed through a Hückel aromatic transition state via a constriction in the orbital topology. Herges called these transformations “coarctate”, meaning compressed or constricted. Although true coarctate reactions are concerted, they cannot be considered pericyclic because bond making and bond breaking do not occur in a cyclic fashion, i.e., the forming or reacting carbene is exocyclic to the five-membered ring. Coarctate reactions can be identified on a visual inspection of the starting materials or products by the coarctate atom(s), the atom(s) at which two bonds are made and two bonds are broken (Figure 2).

With the incorporation of heteroatoms into the ene-ene-yne manifold, there is the potential for lone pair electron participation in the coarctate cyclization, resulting in a pseudocoarctate reaction.^{11,12} If the reaction occurs in the π -framework, there must be distortion from planarity to allow for the orbital overlap necessary for an aromatic transition state; therefore, true coarctate reactions would proceed through non-planar transition states, whereas pseudocoarctate reactions by virtue of the lone pair reactivity would have planar transition states. Furthermore, the pseudocoarctate transition state would be neither aromatic

nor antiaromatic because of a disconnect in the orbital overlap. Thus coarctate reactions exhibit similar mechanistic implications as pericyclic reactions, which are coined pseudopericyclic if there is a “disconnection” in the otherwise contiguous cyclic delocalization of electrons in the transition state. The pericyclic/pseudopericyclic dichotomy has been extensively discussed in the literature.^{12,13}

ACID (anisotropy of the induced current density) is a method developed by the Herges group to visualize the density of electrons that are not localized at an atom or bond but are “mobile” within a molecule if subjected to a magnetic field. ACID is interpreted as the density of delocalized electrons and plotted as an isosurface (similar to the total electron density, yellow surface in Figure 3).¹⁴ Further information about the delocalization of electrons is obtained by plotting the current density on top of the ACID isosurface. The arrows (green arrows with red arrowhead) represent strength and direction of the induced current and thus allow one to differentiate diatropic (aromatic) and paratropic (antiaromatic) ring currents. Application of the ACID method is not restricted to energy minima or ground states, but can also be used to determine the extent and topology of conjugation in transition states. Pericyclic transition states exhibit a cyclic topology of delocalized electrons and a diatropic ring current, which is similar to the π system of aromatics (aromatic transition states).¹⁵ A coarctate reaction is characterized by a hairpin-like pinched cycle in bond making and bond breaking. By visualizing the response of the electrons to the external magnetic field, it is possible to see this “looping” of electrons in an ACID diagram (Figure 3). The ACID method has predictive power, as it defines the extent of conjugation in any kind of structure (ground states, excited states or transition states). It has been applied to linear conjugation, cyclic conjugation, hyperconjugation, aromaticity, homoaromaticity, through bond, through space conjugation and a number of other delocalization effects. More than 50 papers have used ACID to analyze the degree of conjugation including the pericyclic/pseudopericyclic nature of transition states by a number of groups. In the latter case it agrees well with alternative methods like NICS.^{14b}

The ACID method can also be used to distinguish between pericyclic/pseudopericyclic and coarctate/pseudocoarctate.¹⁶ The disconnection in the otherwise contiguous cyclic (pericyclic) or constricted (coarctate) system of delocalized electrons in the transition state, which is characteristic to a pseudo (pericyclic or coarctate) reaction, is clearly visible in the ACID plot as a disconnection of the isosurface. Unfortunately, a disconnection in the context of electron delocalization is not a yes or no question (as it is in simple engineering or electronics). The delocalization of electrons between two parts of a molecule can

(7) Inter alia: (a) Yu, J.; Wearing, X. Z.; Cook, J. M. *J. Org. Chem.* **2005**, *70*, 3963–3979. (b) de Angelis, M.; Stossi, F.; Carlson, K. A.; Katzenellenbogen, B. S.; Katzenellenbogen, J. A. *J. Med. Chem.* **2005**, *48*, 1132–1144. (c) Steffan, R. J.; Matelan, E.; Ashwell, M. A.; Moore, W. J.; Solvibile, W. R.; Trybulski, E.; Chadwick, C. C.; Chippari, S.; Kenney, T.; Ecker, A.; Borger-Marcucci, L.; Keith, J. C.; Xu, Z.; Mosyak, L.; Harnish, D. C. *J. Med. Chem.* **2004**, *47*, 6435–6438. (d) Bentley, K. W. *Nat. Prod. Rep.* **2005**, *22*, 249–268. (e) Tsou, H.-R.; Overbeek-Klumpers, E. G.; Hallett, W. A.; Reich, M. F.; Floyd, M. B.; Johnson, B. D.; Michalak, R. S.; Nilakantan, R.; Discifani, C.; Golas, J.; Rabindran, S. K.; Shen, R.; Shi, X.; Wang, Y.-F.; Upešlacis, J.; Wissner, A. *J. Med. Chem.* **2005**, *48*, 1107–1131. (f) Chauhan, P. M. S.; Martins, C. J. A.; Horwell, D. C. *Bioorg. Med. Chem.* **2005**, *13*, 3513–3518. (g) Li, Z.; Yang, Q.; Qian, X. *Tetrahedron* **2005**, *61*, 8711–8717.

(8) (a) Montes, V. A.; Li, G.; Pohl, R.; Shinar, J.; Anzenbacher, P., Jr. *Adv. Mater.* **2004**, *16*, 2001–2003. (b) Chuen, C. H.; Tao, Y. T.; Wu, F. I.; Shu, C. F. *Appl. Phys. Lett.* **2004**, *85*, 4609–4611. (c) Wu, F.-I.; Su, H.-J.; Shu, C.-F.; Luo, L.; Diau, W.-G.; Cheng, C.-H.; Duan, J.-P.; Lee, G.-H. *J. Mater. Chem.* **2005**, *15*, 1035–1042.

(9) (a) Herges, R. *Angew. Chem., Int. Ed. Engl.* **1994**, *33*, 255–276. (b) Herges, R. *J. Chem. Inf. Comput. Sci.* **1994**, *34*, 91–102.

(10) For a recent review, see: Shirtcliff, L. D.; McClintock, S. P.; Haley, M. M. *Chem. Soc. Rev.* **2008**, *37*, 343–364.

(11) Ross, J. A.; Seiders, R. P.; Lemal, D. M. *J. Am. Chem. Soc.* **1976**, *98*, 4325–4327.

(12) (a) Birney, D. M.; Ham, S.; Unruh, G. R. *J. Am. Chem. Soc.* **1997**, *119*, 4509–4517. (b) Birney, D. M.; Wagenseller, P. E. *J. Am. Chem. Soc.* **1994**, *116*, 6262–6270. (c) Birney, D. M. *J. Org. Chem.* **1996**, *61*, 243–251. (d) Birney, D. M. *Org. Lett.* **2004**, *6*, 851–854. (e) Birney, D. M.; Xu, X.; Ham, S. *Angew. Chem., Int. Ed.* **1999**, *38*, 189–193.

(13) (a) Subbotina, J. O.; Sadchikova, E. V.; Bakulev, V. A.; Fabian, W. M. F.; Herges, R. *Int. J. Quantum Chem.* **2007**, *107*, 2479–2488. (b) Chamorro, E.; Notario, R.; Santos, J. C.; Pérez, P. *Chem. Phys. Lett.* **2007**, *443*, 136–140. (c) Rodríguez-Otero, J.; Cabaleiro-Lago, E. M.; Hermida-Ramon, J. M.; Pena-Gallego, A. *J. Org. Chem.* **2003**, *68*, 8823–8830. (d) Zhou, C.; Birney, D. M. *J. Am. Chem. Soc.* **2002**, *124*, 5231–5241. (e) Pena-Gallego, A.; Rodríguez-Otero, J.; Cabaleiro-Lago, E. M. *J. Org. Chem.* **2004**, *69*, 7013–7017.

(14) (a) Herges, R.; Geuenich, D. *J. Phys. Chem. A* **2001**, *105*, 3214–3220. (b) Geuenich, D.; Hess, K.; Kohler, F.; Herges, R. *Chem. Rev.* **2005**, *105*, 3758–3772.

(15) Herges, R.; Jiao, H.; Schleyer, P. v. R. *Angew. Chem., Int. Ed. Engl.* **1994**, *33*, 1376–1378.

(16) (a) Pena-Gallego, A.; Rodríguez-Otero, J.; Cabaleiro-Lago, E. M. *J. Org. Chem.* **2004**, *69*, 7013–7017. (b) Rodríguez-Otero, J.; Cabaleiro-Lago, E. M.; Hermida-Ramon, J. M.; Pena-Gallego, A. *J. Org. Chem.* **2003**, *68*, 8823–8830. (c) Subbotina, J. O.; Bakulev, V. A.; Herges, R.; Fabian, W. M. F. *Int. J. Quantum Chem.* **2006**, *106*, 2229–2235.

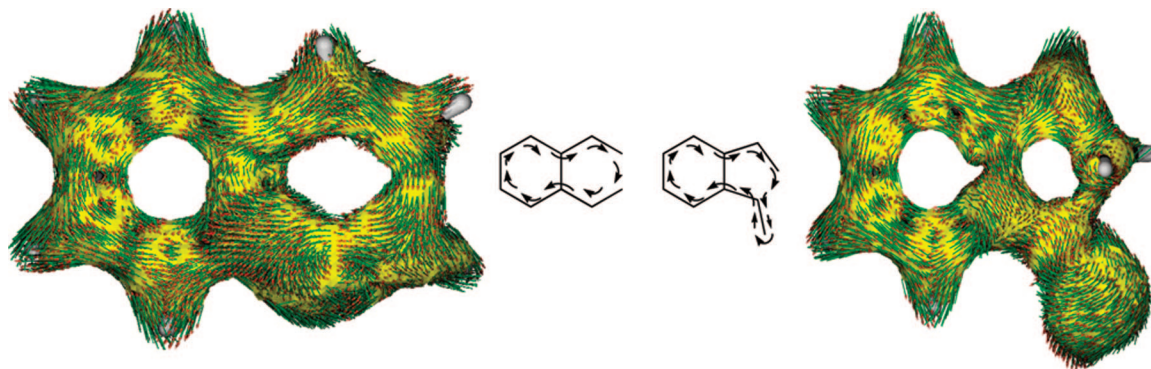


FIGURE 3. Electron flow in the non-planar TS of a pericyclic (left) and coarctate (right) reaction of *o*-ethynylstyrene (Figure 5) with ACID plots taken at isosurface value of 0.05. The vector field of the induced current density depends on the relative orientation of the molecule with respect to the magnetic field. The magnetic field in all plots is orthogonal with respect to the benzene ring. The scale (length of the arrows) is a function of the strength of the induced current at the point of origin of the arrow. The scale is the same for all ACID plots.

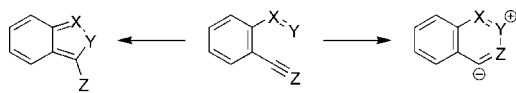


FIGURE 4. Design of heteroatom variations for the dual cyclization of benzo-fused ene-ene-yne systems.

be anywhere between strong and none, depending on the structural and electronic conditions. To quantify the degree of electron delocalization, we defined the so-called “critical isosurface value” (CIV). The CIV is the ACID value (density of delocalized electrons) at the point of the lowest delocalization in a conjugated system (for a mathematical definition see ref 14b).¹⁴ Applied to transition states of pericyclic and coarctate reactions, the CIV gives a number that determines the degree of disconnection (a CIV of zero would imply a perfect disconnection of electron delocalization and thus a perfect pseudo type reaction). We define pericyclic and coarctate reactions with a CIV value below 0.025 as a pseudo-type reaction, while values above 0.03 are taken as the true form. Values in between are classified as borderline.³ Of course such definitions are always somewhat arbitrary; however, these values approximately match the classification that has been discussed in the literature for pseudo(pericyclic) reactions using various other parameters.^{3,12,13}

Given our prior successes with benzo-fused azo-ene-yne, a systematic study of activation barriers as a result of the nature and position of the heteroatoms (X, Y, Z) could be used to design new reactions and to identify promising candidates for further experimental inquiry (Figure 4). In this paper we present computational findings in our ongoing effort to design new reactions which yield benzo-fused five- or six-membered rings arising from conjugated ene-ene-yne precursors. The influence of heteroatoms on the overall reaction energetics has been studied by varying the atom in the bond making position, as well as by varying the position of the heteroatom within the ene-ene-yne moiety.

Results and Discussion

Computational Methods. All computations were calculated using the Gaussian 98¹⁷ or 03¹⁸ suite of programs at the B3LYP/6-31G* level of theory. This has proven to be a good compromise between the computational cost and accuracy of previously investigated azo-ene-yne cyclizations where the computed activation barriers and the experimental conditions were in reasonable agreement.^{1b,c,2–4} All stationary points were

confirmed by harmonic frequency analysis and checked for stability for triplet and SCF convergence. The energies of the stationary points were determined, including zero point energies at the same level of theory. ACID calculations were performed using the previously reported method of Herges et al.,¹⁴ with the ACID scalar fields interpreted as the density of delocalized electrons.

Parent Hydrocarbon. The general energy profile for the cyclization of the parent ene-ene-yne hydrocarbon, *o*-ethynylstyrene (**5**), is shown in Figure 5. Before cyclization is possible, **5** must undergo rotation about the vinyl-phenyl bond to assume reactive conformation **6**. In this conformation, **6** can undergo a pericyclic reaction to give **7** by way of transition state **8**. The pericyclic product can either be allenic (as in **7**) or zwitterionic as shown in Figure 6; however, the zwitterionic structure is important (contributing to the wave function) only if a heteroatom participates in the bond making. Compound **6** can also undergo a coarctate reaction to give carbenes **9** or **10** with the difference being the orientation of the hydrogen relative to the original aryl ring. Cyclized product **9** is oriented such that the hydrogen is *syn* to the ring, while **10** is in *anti* conformation. These compounds come from the corresponding coarctate transition states **11** and **12**. In the initial triazene-ene-yne studies

(17) Frisch, M. J.; Trucks, G. W.; Schlegel, H. B.; Scuseria, G. E.; Robb, M. A.; Cheeseman, J. R.; Zakrzewski, V. G.; Montgomery, J. A.; Stratmann, R. E.; Burant, J. C.; Dapprich, S.; Millam, J. M.; Daniels, A. D.; Kudin, K. N.; Strain, M. C.; Farkas, O.; Tomasi, J.; Barone, V.; Cossi, M.; Cammi, R.; Mennucci, B.; Pomelli, C.; Adamo, C.; Clifford, S.; Ochterski, J.; Petersson, G. A.; Ayala, P. Y.; Cui, Q.; Morokuma, K.; Rega, N.; Salvador, P.; Dannenberg, J. J.; Malick, D. K.; Rabuck, A. D.; Raghavachari, K.; Foresman, J. B.; Cioslowski, J.; Ortiz, J. V.; Baboul, A. G.; Stefanov, B. B.; Liu, G.; Liashenko, A.; Piskorz, P.; Komaromi, I.; Gomperts, R.; Martin, R. L.; Fox, D. J.; Keith, T.; Al-Laham, M. A.; Peng, C. Y.; Nanayakkara, A.; Challacombe, M.; Gill, P. M. W.; Johnson, B.; Chen, W.; Wong, M. W.; Andres, J. L.; Gonzalez, C.; Head-Gordon, M.; Replogle, E. S.; Pople, J. A. *Gaussian 98, Revision A.11.4*; Gaussian, Inc.: Pittsburgh, PA, 2002.

(18) Frisch, M. J.; Trucks, G. W.; Schlegel, H. B.; Scuseria, G. E.; Robb, M. A.; Cheeseman, J. A.; Vreven, T.; Kudin, K. N.; Burant, J. C.; Millam, J. M.; Iyengar, S. S.; Tomasi, J.; Barone, V.; Mennucci, B.; Cossi, M.; Scalmani, G.; Rega, N.; Petersson, G. A.; Nakatsuji, H.; Hada, M.; Ehara, M.; Toyota, K.; Fukuda, R.; Hasegawa, J.; Ishida, M.; Nakajima, T.; Honda, Y.; Kitao, O.; Nakai, H.; Klene, M.; Li, X.; Knox, J. E.; Hratchian, H. P.; Cross, J. B.; Adamo, C.; Jaramillo, J.; Gomperts, R.; Stratmann, R. E.; Yazyev, O.; Austin, A. J.; Cammi, R.; Pomelli, C.; Ochterski, J. W.; Ayala, P. Y.; Morokuma, K.; Voth, G. A.; Salvador, P.; Dannenberg, J. J.; Zakrzewski, V. G.; Dapprich, S.; Daniels, A. D.; Strain, M. C.; Farkas, O.; Malick, D. K.; Rabuck, A. D.; Raghavachari, K.; Foresman, J. B.; Ortiz, J. V.; Cui, Q.; Baboul, A. G.; Clifford, S.; Cioslowski, J.; Stefanov, B. B.; Liu, G.; Liashenko, A.; Piskorz, P.; Komaromi, I.; Martin, R. L.; Keith, T.; Al-Laham, M. A.; Peng, C. Y.; Nanayakkara, A.; Challacombe, M.; Gill, P. M. W.; Johnson, B.; Chen, W.; Wong, M. W.; Gonzalez, C.; Pople, J. A. *Gaussian 03, Revision B.04*; Gaussian, Inc.: Pittsburgh, PA, 2003.

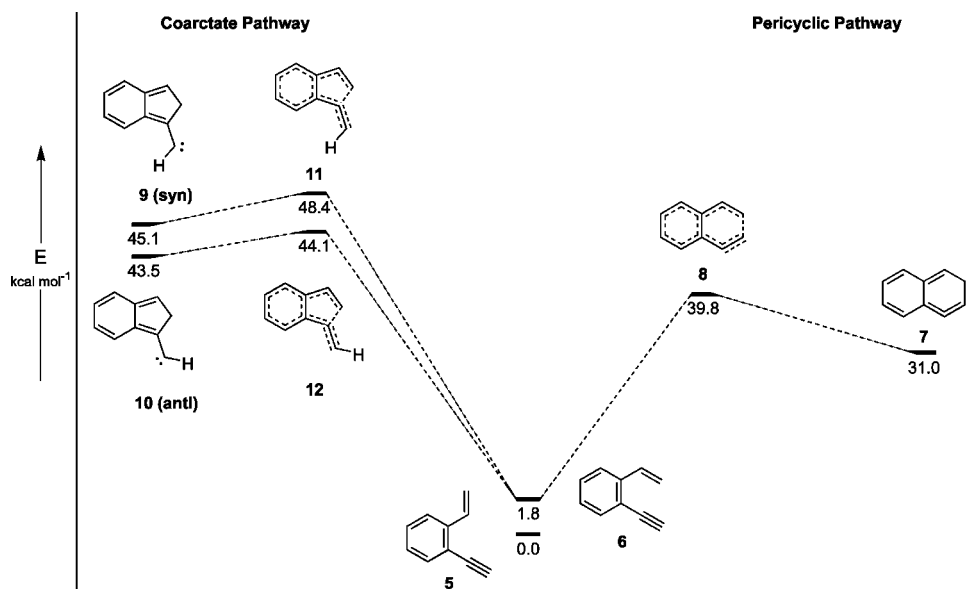


FIGURE 5. DFT (B3LYP/6-31G*+ZPE) calculated relative energies for the dual cyclization pathways of *o*-ethynylstyrene (**5**).

TABLE 1. Effect of Atoms in the Bond Making Position on Cyclization^a

compd	Y	reactive conformation	<i>syn</i> product ^b	<i>anti</i> product ^b	pericyclic product	<i>syn</i> TS	<i>anti</i> TS	peri TS
6	CH ₂	1.8	45.1	43.5	31	48.4	44.1	39.8
13	NH	3.9	17	19.4	7.6	31.3	26.8	24.5
14	O	2.4	39.4	<i>c</i>	29.9	40.3	na	31.4
15	S	4.5	27.1	24.6	19.4	35.1	24.7	22.1

^a Calculated energies (B3LYP/6-31G*) in kcal mol⁻¹. ^b Orientation refers to the hydrogen on the carbene atom relative to the phenyl ring (Figure 7). ^c No energy minimum found.

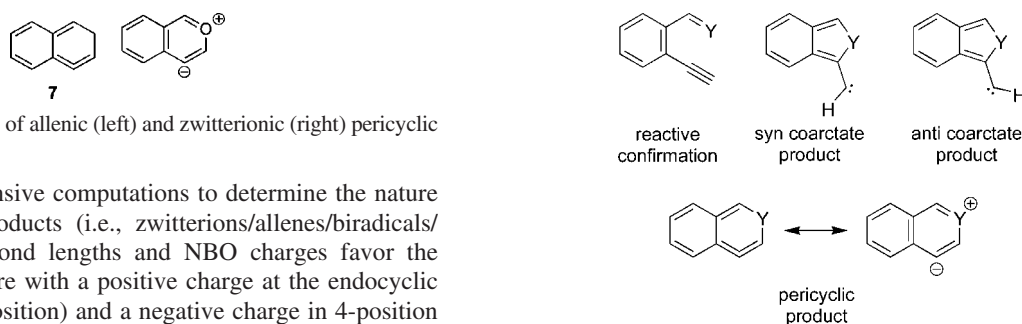


FIGURE 6. Examples of allenic (left) and zwitterionic (right) pericyclic products.

we performed extensive computations to determine the nature of the cyclized products (i.e., zwitterions/allenes/biradicals/carbenes).^{1b} The bond lengths and NBO charges favor the zwitterionic structure with a positive charge at the endocyclic nitrogen atom (2-position) and a negative charge in 4-position of the cinnoline ring system. The all-carbon system, according to the NBO analysis, does not exhibit distinct partial charges, neither in the transition state nor in the pericyclic product. Studies to find biradical structures on the reaction hypersurface all resulted in collapse into the corresponding closed shell systems.

Unsubstituted Ene-Ene-Yne Cyclizations. We first examined the effect on reaction energetics by exchanging the vinylidene unit with isoelectronic heteroatomic fragments (Figure 7 and Table 1). Moving across the periodic row reveals no discernible trends, with **6** (carbon) having the highest energies, followed by aldehyde **14** (oxygen) and imine **13** (nitrogen). The *syn* carbene product of alkene **6** lies 1.6 kcal mol⁻¹ higher in energy than the *anti* product; conversely, the *anti* product of **13** is 2.4 kcal mol⁻¹ higher than the *syn*. Aldehyde **14** yields only one energy minimum for the coarctate cyclizations, where all attempts to find a stationary structure for the *anti* carbene were unsuccessful. In general, the pericyclic cyclizations have lower activation energies than the coarctate reactions. This is somewhat unexpected since the pericyclic

FIGURE 7. Variation of the ene-ene-yne system (Y = CH₂, NH, O, S).

cyclizations in previously investigated systems proceeded via a thermodynamic pathway (higher TS energy and lower product energy) compared to the coarctate reaction.¹ The coarctate cyclization of **14** has only a 0.9 kcal mol⁻¹ energy difference between the product and transition state, and is endothermic by 29.9 kcal mol⁻¹ which indicates that the proposed cyclization should be unfavored and reversible. Imine **13** sees the greatest energy difference between TS and products with 14.3, 7.4, and 16.9 kcal mol⁻¹ energy stabilization for the *syn*, *anti*, and pericyclic products, respectively. Switching from aldehyde **14** to thioaldehyde **15** results in the reduction of activation barriers and formation of lower energy products (Table 1).

Analysis of the transition states reveals that both of the CH₂-terminated ene-ene-yne cyclizations (five-membered ring and six-membered ring formation) are truly coarctate and pericyclic, respectively, as would be expected with no lone pair electrons available. The transition states are both non-planar (Table 2)

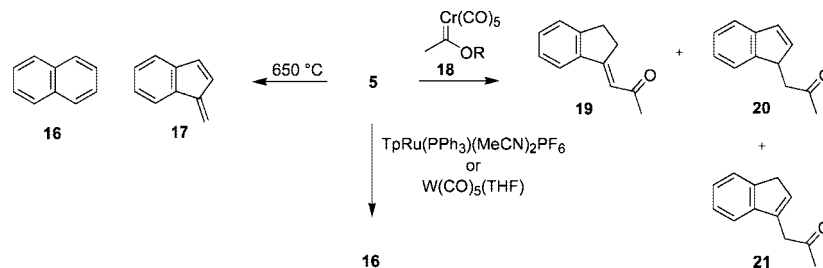
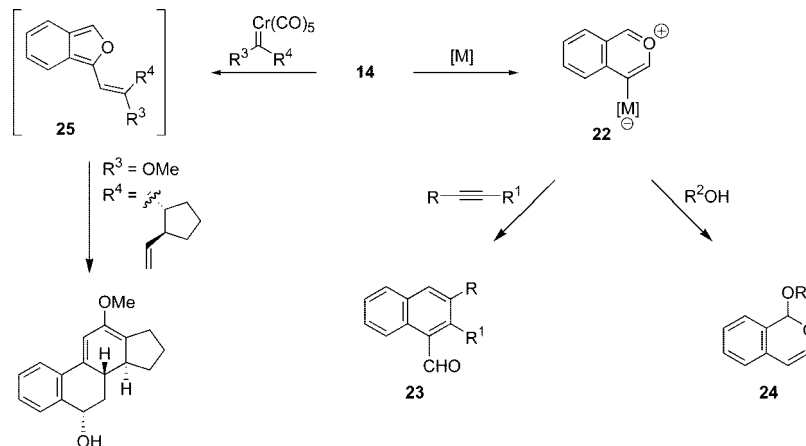
SCHEME 1. Experimental Cyclizations of **6**SCHEME 2. Known Cyclization Reactions of **14**

TABLE 2. Dihedral Angle and ACID CIV Analysis of the Transition State Structures

compd	Y	syn		peri	
		angle ^a	CIV ^b	angle ^a	CIV ^b
6	CH ₂	16.72	0.0598	12.82	0.0743
13	NH	0.01	0.0238	0.00	0.0206
14	O	0.01	0.0371	0.00	0.0375
15	S	0.00	0.0311	0.02	0.0317



^a Dihedral angle defined as $\angle a-b-d-e$. ^b Blue indicates π reactivity, red indicates lone pair reactivity.

and have CIVs well over the 0.03 threshold. Upon moving to the heteroatom-terminated systems, however, the transition states are all planar, which would indicate that the lone pairs are participating in the reactions. The transition states of the cyclizations of imine **13** have CIVs of 0.0238 and 0.0206, both below the 0.025 threshold, meaning they are pseudocoarctate and pseudopericyclic reactions, respectively. Aldehyde **14** and thioaldehyde **15**, however, have CIVs in their transition states above 0.03 suggesting more delocalization in the transition state typical of a true coarctate reaction. This is due to the fact that the transition state is product-like and being an isobenzofuran, it is fully conjugated without a disconnection. Therefore, both the π orbital and the lone pair at oxygen are participating in the bond forming process even though the TS is planar. The effect is less pronounced in the case of **13** because the reaction is less endothermic and the TS less product-like.

Examination of the transition states using ACID plots shows increased delocalization for **6** compared to **13** (Figure 8). With CIVs of 0.0598 and 0.0238, respectively, it is easy to see a clear distinction in the ACID plots between a coarctate reaction,

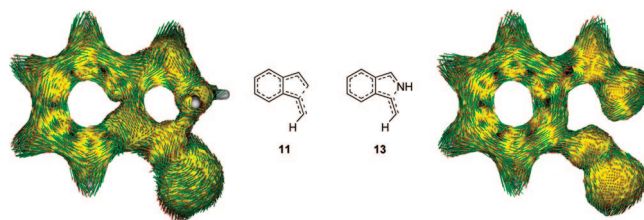


FIGURE 8. ACID plots of the transition states for the cyclization of **6** and **13** taken at an isosurface value of 0.05. The cyclization of **6** is truly coarctate (CIV = 0.0598), whereas the reaction of **13** is pseudocoarctate (CIV = 0.0238). Transition state **11** exhibits a contiguous system of delocalized electrons, and there is a clear disconnection in the transition structure of **13** between the two bond-forming atoms.

which has extensive delocalization (**6**, TS **11** shown), compared to the pseudocoarctate reaction which does not (**13**). The lower arms of the molecules reveal a looping of electrons and formation of a carbene, characteristics indicative of coarctate-style reactivity. The thermal cyclization of **6** has been examined using the electron localization function (ELF) by Cárdenas et al.¹⁹ It was determined that **6** cyclizes in a "true" coarctate and pericyclic pathway, which is in good agreement with our ACID results.

Examination of the literature suggests that there has been experimental precedent for these cyclizations for some time now. The thermal or transition metal mediated cyclization of **6** has yielded both the coarctate and pericyclic products in varying yields (Scheme 1).^{18–24} The pyrolysis of **6** at 650 °C in an oxygen free environment yielded naphthalene (**16**) and indene (**17**) derivatives, which were proposed to arise from three competing pathways, an electrocyclic reaction, a carbene

(19) Cárdenas, C.; Chamorro, E.; Notario, R. *J. Phys. Chem. A* **2005**, *109*, 4352–4358.

TABLE 3. Energies of N-Substitution of Imine-Ene-Yne Cyclizations^a

compd	R	reactive conformation ^b	syn product ^b	anti product ^b	pericyclic product ^b	syn TS	anti TS	peri TS
13	H	3.9	17	19.4	7.6	31.3	26.8	24.5
26	Ph	3.6	22.2	23.7	12.4	30.2	26.4	24.7
27	NH ₂	3.6	18.3	25.7	14.7	27.8	29.8	28.8

^a Calculated energies (B3LYP/6-31G*) in kcal mol⁻¹. ^b Molecule orientations as shown in Figure 9.

TABLE 4. Cyclizations of Nitrogen-Containing Ene-Ene-Yne Systems^a

compd	Y	Z	reactive conformation ^b	syn product ^b	anti product ^b	pericyclic product ^b	syn TS ^b	anti TS ^b	peri TS ^b
30	CH ₂	CH	0.3 ^c	27.8	27.1	21.1	42.9	34.7	34.4
31	CH(Ph)	CH	0.5 ^c	38.8	37.8	39.1	51.3	41.2	40.0
1 ^d	N(NH ₂)	CH	2.3	18.0	26.1	13.2	27.6	29.6	29.6
32	PH	CH	0.3	19.4	17.5	15.0	^e	19.2	18.8
33	O	CH	1.3	20.4	18.1	13.2	26.7	21.3	24.5
34	O	N	1.0	22.2 ^f	^e	28.9 ^f	NA		

^a Calculated energies (B3LYP/6-31G*) in kcal mol⁻¹. ^b Molecule orientation as shown in Figure 10. ^c Non-planar conformation. ^d Reference 1b. ^e No stationary point found. ^f Nitroso-ene-nitrile cyclization yields a nitrene that has only one conformation; calculated using UB3LYP/6-31G* as a triplet nitrene.

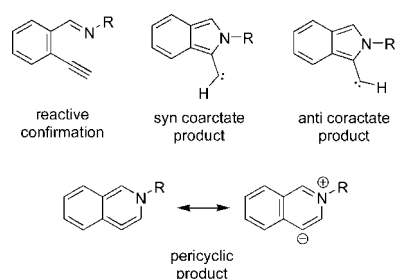


FIGURE 9. N-Substitution of imine-ene-yne cyclization.

reaction, and a radical reaction.²⁰ Treatment of **6** with Fischer carbene **18** furnished Indane **19** and indenenes **20** and **21** resulting from a “formal” coarctate cyclization.²¹ Ru²² and W²³ catalysts have been able to transform **6** to naphthalene in yields of 95% and 68%, respectively; however, when using transition metal complexes, the exact mechanism(s) may become more complicated and the cyclizations are only formally coarctate or pericyclic.

While carbonyl-ene-yne systems have been well documented in the literature,¹⁰ the corresponding phenyl based al-ene-yne cyclizations have received less attention. There have been several examples, however, that show the versatility of these ring-forming reactions (Scheme 2). Treatment of **14** with Au,²⁵ Cu,^{26,27} W,²⁸ or Pd²⁹ catalysts results in six-membered ring formation where the resulting metal-stabilized zwitterionic

(20) Hofmann, J.; Schultz, K.; Altmann, A.; Findeisen, M.; Zimmermann, G. *Liebigs Ann./Recueil* **1997**, 2541–2548.

(21) Zhang, L.; Herndon, J. W. *Organometallics* **2004**, 23, 1231–1235.

(22) Shen, H. C.; Pal, S.; Lian, J. J.; Liu, R. S. *J. Am. Chem. Soc.* **2003**, 125, 15762–15763.

(23) Maeyama, K.; Iwasawa, N. *J. Org. Chem.* **1999**, 64, 1344–1346.

(24) For several examples of non-benzo fused ene-ene-yne cyclizations, see: (a) Roth, W. R.; Hopf, H.; Horn, C. *Chem. Ber.* **1994**, 127, 1765–1779. (b) Nuchter, U.; Zimmermann, G.; Francke, V.; Hopf, H. *Liebigs Ann./Recueil* **1997**, 1505–1515. (c) Hopf, H.; Berger, H.; Zimmermann, G.; Nuchter, U.; Jones, P. G.; Dix, I. *Angew. Chem., Int. Ed. Engl.* **1997**, 36, 1187–1190. (d) Zimmermann, G. *Eur. J. Org. Chem.* **2001**, 45, 7–471.

(25) Asao, N.; Takahashi, K.; Lee, S.; Kasahara, T.; Yamamoto, Y. *J. Am. Chem. Soc.* **2002**, 124, 12650–12651.

(26) Asao, N.; Kasahara, T.; Yamamoto, Y. *Angew. Chem., Int. Ed.* **2003**, 42, 3504–3506.

(27) Patil, N. T.; Yamamoto, Y. *J. Org. Chem.* **2004**, 69, 5139–5142.

(28) Kasama, H.; Funami, H.; Shido, M.; Hara, Y.; Takaya, J.; Iwasawa, N. *J. Am. Chem. Soc.* **2005**, 127, 2709–2716.

(29) Asao, N.; Nogami, T.; Takahashi, K.; Yamamoto, T. *J. Am. Chem. Soc.* **2002**, 124, 764–765.

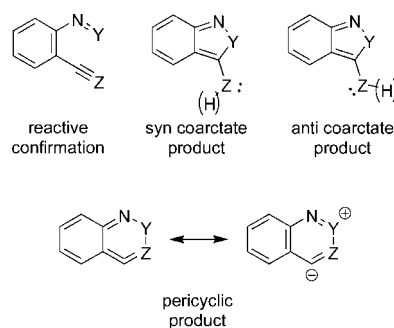


FIGURE 10. Structures of imine/nitroso-ene-yne systems.

intermediates (**22**) are trapped via either Diels–Alder cycloadditions^{25,26,28} or nucleophiles^{27,29} to give a range of cyclic products (e.g., **23**, **24**). Similar to their work with **6**, Herndon and co-workers have been interested in the cyclization of **14**. While the exact mechanism is likely more complicated due to the use of a Fischer carbene, the reaction can nonetheless be seen as a formal coarctate cyclization that proceeds through intermediate **25**.^{30–34} Despite the success of **14**, there are currently no example systems similar to **13** or **15** undergoing these types of reactions even though they have lower cyclization energies.

Substituted Imine-Ene-Yne Cyclizations. Substituents on the bond making atom were also investigated to determine the effect that electron donating or withdrawing groups have on the overall cyclization energies (Figure 9 and Table 3). Changing from **13** (NH) to NPh- or NNH₂-terminated ene-ene-yne systems (**26** and **27**, respectively) results in almost no difference in the reactive conformation energies; however, substitution results in higher product energies presumably due to increased steric congestion. Imine **26** experiences an overall decrease in energies for the coarctate transition states by 1.1 and 0.4 kcal mol⁻¹ while

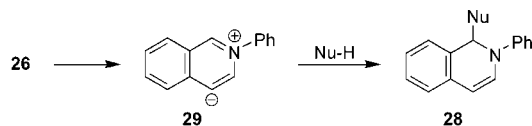
(30) Ghorai, B. K.; Herndon, J. W.; Lam, Y. F. *Org. Lett.* **2001**, 3, 3535–3538.

(31) Li, R.; Zhang, L.; Camacho-Davila, A.; Herndon, J. W. *Tetrahedron Lett.* **2005**, 46, 5117–5120.

(32) Ghorai, B. K.; Menon, S.; Johnson, D. L.; Herndon, J. W. *Org. Lett.* **2002**, 4, 2121–2124.

(33) Menon, S.; Sinha-Mahapatra, D.; Herndon, J. W. *Tetrahedron* **2007**, 63, 8788–8793.

(34) Ghorai, B. K.; Jiang, D.; Herndon, J. W. *Org. Lett.* **2003**, 5, 4261–4263.

SCHEME 3. Pericyclic Reactivity of **26**

the pericyclic transition state is 0.2 kcal mol⁻¹ higher than **13**. Hydrazone **27** has a higher transition state energy for the *anti* (3.0 kcal mol⁻¹) and pericyclic (4.3 kcal mol⁻¹) cyclizations with a lower activation barrier for the *syn* (3.5 kcal mol⁻¹) product.

Experimentally, cyclization of **26** has been found to be a good method for the synthesis of 1,2-dihydroisoquinolines (**28**, Scheme 3), while the coarctate cyclization pathway has not been observed. This is in agreement with the higher barriers for the five-membered ring cyclization. Treatment of **26** with pronucleophiles (Nu-H) both with and without catalysts has resulted in pericyclic reactivity.^{35–38} In situ generation of the imine via the condensation of **14** and aniline in the presence of CHCl₃ as the pronucleophile afforded a 91% yield of **28** (Nu = CCl₃) after 48 h in the presence of only molecular sieves.³⁵ The cyclization can be catalyzed by Ag, Au, or In salts, which activate the alkyne and stabilize the resulting zwitterions.^{36–38} A variety of pronucleophiles have been used, including nitromethane, terminal alkynes, allyl-metal complexes, silyl-vinyl ethers, and vinyl boronic acids. There have been no examples of hydrazone **27** undergoing this type of reactivity.

Imine/Nitroso-Ene-Yne Cyclizations. The success of our azo-ene-yne cyclization studies led us to explore the viability of changing one of the nitrogen atoms of the azo linkage to still give experimentally accessible systems. Imines **30** and **31** (Figure 10, Table 4) have a carbon in the bond-making position. The hydrogen atoms at the carbon force the system to twist slightly out of plane to decrease interactions between the hydrogen and the acetylene unit. In this series, the coarctate products in the *anti* orientation all have a lower energy than the corresponding *syn* products by 0.7–2.3 kcal mol⁻¹. With the exception of **31**, coarctate reactions give higher energy products than the pericyclic cyclization. The transition state energies follow the same trend as the products with the *anti* conformations being lower in energy than the *syn*; however, there is a much larger (5–10 kcal mol⁻¹) energy difference between the two transition state conformations.

The imines experience an overall increase in the relative energies when going from **30** to **31**. As with the previous systems, incorporation of a heteroatom in the bond making position results in a lowering of energies, with this being most prominent in the transition states. A carbon in the bond making position results in transition states that are quite high in energy while the hetero systems have energies that are much lower.

The transition states reveal high CIVs and non-planarity for **30** and **31**, which classify the five- and six-membered ring-forming reactions for both as coarctate and pericyclic, respectively (Table 5). Phosphorus-containing **32** is unusual in that it has a non-planar transition state and CIV above 0.03 for the coarctate cyclizations, both of which indicate that the lone pair

TABLE 5. Transition State Analysis for Nitrogen Containing Ene-Ene-Yne Systems

compd	Y	Z	<i>syn</i>		<i>peri</i>	
			angle ^a	CIV ^b	angle ^a	CIV ^b
30	CH ₂	CH	14.05	0.0713	12.28	0.0697
31	CH(Ph)	CH	14.32	0.0721	6.02	0.0764
1^c	N(NH ₂)	CH	6.37	0.028	6.38	0.045
32	PH	CH	23.89 ^d	0.0356 ^d	3.00	0.0259
33	O	CH	0.03	0.0670	0.00	0.0409
34	O	N	0.00	0.0304	–	–

^a Dihedral angle defined as ∠a–b–d–e. ^b Blue indicates π reactivity; red indicates lone pair reactivity. ^c Reference 1b. ^d Data given for *anti* orientation as no transition state was found for the *syn*.

electrons are not participating. This is the only case where a cyclization containing a heteroatom in the bond making position is clearly proceeding through a true coarctate pathway. The pericyclic reaction on the other hand has a non-planar transition state with a borderline CIV, which would suggest as well that it is a true pericyclic reaction. In nitroso systems **33** and **34** there is again the ambiguity in the classifications as both have planar transition states but high CIVs. This would indicate that the transition states are delocalized regardless of the planar transition states, which is unexpected at first glance. However, the more endothermic the reaction is, the more product-like is the transition state. If the product is aromatic, the CIV therefore of course is also large in the TS, because the CIV is due to a simple (product-like) aromatic conjugation (which should not be confused with the conjugation due to the electrons participating in the reaction). The product is aromatic only if Y (Table 5) is a heteroatom. That is why we find considerable CIVs even in planar transition states in the “hetero cases”. In the Y = CH₂ system the methylene group in the product prevents cyclic conjugation. On the other hand, the hydrogens at the CH₂ group prevent a planar (pseudo) transition state. In this case the large CIV is due to a genuine TS delocalization. However, planarity dictates that the π orbitals are not able to overlap, and therefore the lone pair electrons must be participating in the reactions. Triazene **1** has also been examined using ELF and determined that both cyclization pathways exhibit a disconnection in the otherwise contiguous delocalization of electrons in the transition state and thus are pseudocoarctate and pseudopericyclic,¹⁹ in agreement with our findings.

Based on the promising energy profile for **34**, our laboratory has recently examined the reactivity experimentally.³⁹ Using tetramethylethylene as a nitrene/nitrenium trap, however, resulted in a nitroso-ene reaction (**35**) followed by an intramolecular cyclization (**36**, Scheme 4). Under all reaction conditions attempted, no pseudocoarctate reactivity was observed, which indicates that while the calculated energy profile appeared promising, the nitroso-ene reaction was a more favorable pathway. Imine **31** was investigated experimentally in our laboratory but failed to undergo the desired reactions. None of the other calculated system have yet been investigated.

Triplet calculations were performed for all products of the 5-ring (carbenes) and 6-ring (zwitterionic) cyclizations (see

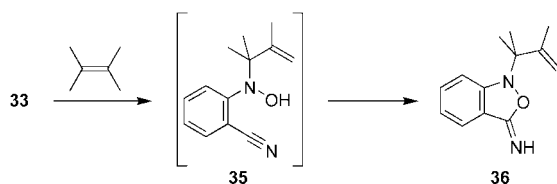
(35) Asao, N.; Iso, K.; Yudha, S. S. *Org. Lett.* **2006**, *8*, 4149–4151.

(36) Asao, N.; Yudha, S. S.; Nogami, T.; Yamamoto, Y. *Angew. Chem., Int. Ed.* **2005**, *44*, 5526–5528.

(37) Yanada, R.; Obika, S.; Kono, H.; Takemoto, Y. *Angew. Chem., Int. Ed.* **2006**, *45*, 3822–3825.

(38) Obika, S.; Kono, H.; Yasui, Y.; Yanada, R.; Takemoto, Y. *J. Org. Chem.* **2007**, *72*, 4462–4468.

(39) Jeffrey, J. L.; McClintock, S. P.; Haley, M. M. *J. Org. Chem.* **2008**, *73*, 3288–3291.

SCHEME 4. Unanticipated Reactivity of **33**

Supporting Information). As expected, the singlet of the carbenes are stabilized, if the empty p orbital at the carbene center is conjugated with the electron rich pi system of the aromatic heterocycle, which is formed during cyclization. For example, if Y = N (**13**, **27**), the singlet–triplet splitting is larger than 7 kcal mol⁻¹ in favor of the singlet. With Y = O and S the splitting is small and within the limits of accuracy of the theoretical method. For Y = CCH₂ or CH(Ph) (**5**, **30** and **31**), the 5-ring cyclization product is not aromatic and the ground-state of the carbene is triplet. A similar trend holds for the singlet triplet splitting of the 6-ring cyclization products. If Y is a first row heteroatom the structures are closed shell singlets. In all other cases they are probably triplet ground states or singlet diradicaloids.

Conclusion

We performed theoretical calculations to design new reactions for the synthesis of heterocyclic compounds, as well as elucidate the mechanism and predict scope/limitation of these novel and synthetically useful cyclizations. Like previously investigated systems, both the coarctate as well as pericyclic cyclizations are concerted and both primary products, the carbene and the zwitterion (or cyclic allene), are high in energy. Hence, both reactions are endothermic, the transition states are product-like, and the reactions are reversible. The transition state is lower in energy if the product is stabilized by aromaticity.⁴⁰ This is the case if the atom attacking the triple bond is a heteroatom whose lone pair complements the cyclic delocalization in the product. Likewise, the more nucleophilic the attacking heteroatom, the lower the barrier of the reaction. The investigated set of reactions

(40) For another example of aromatic stabilization of transition states, see: Navarro-Vazquez, A.; Prall, M.; Schreiner, P. R. *Org. Lett.* **2004**, *6*, 2981–2984.

spans the range from purely nonpolar coarctate/pericyclic cyclizations to a more polar, pseudocoarctate/pseudopericyclic addition to the triple bond. Since the reactions (five- and six-membered ring formation) are reversible in the first step, the coarctate cyclization can be favored by stabilizing or trapping the carbene product. This would explain the experimental successes observed when using Cu(I) and Rh(II) catalysts.

This computational study also reveals some ambiguity in the classification of these unusual reactions, in particular, the role that the lone pair electrons play. Analysis of the transition states reveals planarity in a majority of the structures that indicates that the lone pairs and not the π electrons are reacting. ACID analysis, however, often shows a great deal of delocalization, which is indicative of π orbital overlap. It would seem that the geometry constraints would make the π reactivity unlikely and the high degree of delocalization is a result of transition states which are very close in energy to an aromatic product and therefore very product-like. The rather strong and contiguous cyclic delocalization (high CIV) in these planar TS structures is due to the aromatic, product-like π system and does not result from an intrinsic aromaticity of the TS.

This study suggests that the hydrazone **27** and N=P containing **32** have promising energy profiles that make them viable candidates for experimental examination. We hope that this computational design will inspire others to study these unusual cyclization reactions. While there has been some experimental inquiry into these reactions, the scope and limitations of these cyclizations (especially the relatively new coarctate cyclization) is far from being completely explored. Additional examples are currently under investigation in our laboratory.

Acknowledgment. We thank the National Science Foundation (CHE-0718242) and the Fonds der Chemischen Industrie for support of this research. L.D.S. and S.P.M. acknowledge the NSF-IGERT program (DGE-0114419 and 0549503, respectively) for fellowships and travel support to Germany.

Supporting Information Available: All computational details including Cartesian coordinates, total energies and imaginary frequencies for all computed structures. This material is available free of charge via the Internet at <http://pubs.acs.org>.

JO801390X